Time-Varying Techniques for Multisensor Signal Detection

Kofi Ghartey, Antonia Papandreou-Suppappola, *Senior Member, IEEE*, and Douglas Cochran, *Senior Member, IEEE*

***Abstract*—In source detection and localization, the presence of a common but unknown signal can be detected from several noisy sensor measurements using the generalized coherence (GC) estimate. We propose to improve the performance of the GC estimate for multisensor detection using noise-suppressed signal estimates obtained from time-varying techniques. If one of the sensors has a significantly higher signal-to-noise ratio (SNR) than the other sensors, then it could be preprocessed prior to the GC estimate to improve detection performance for the remaining, lower SNR sensors. We perform this processing by estimating time-varying signals of interest with nonlinear phase functions using two methods: a) a modified matching pursuit decomposition (MMPD) algorithm whose dictionary is similar, in time-frequency structure, to the signal and b) an instantaneous frequency (IF) estimation method using highly localized time-frequency representations. The MMPD can yield signal estimates with lower mean square errors than the IF estimation technique but at the expense of higher computational cost and memory requirements. Using simulations, we compare the performance of the GC estimate with the significantly improved performance of the GC estimate that employs the signal estimate from the high SNR sensor. For the two-sensor detection, the estimated signal is also used with a generalized likelihood ratio test statistic to further improve performance.**

***Index Terms*—Generalized coherence estimate, instantaneous frequency (IF) estimation, multisensor detection, time–frequency representations.**

I. Introduction

With recent advances in network technologies, multisensor signal processing has become increasingly relevant for source detection and localization in numerous applications such as remote sensing, radar, sonar, communications, and biomedical diagnosis. Often, a common but unknown signal is to be detected and its source located using noisy data collected from two or more spatially distributed sensors. A common statistic for two-sensor detection is the magnitude-squared coherence (MSC) estimate that provides a measure of similarity between the received data from the two sensors [1]–[3].

The MSC estimate was extended to an L-sensor detection system, forming the generalized coherence (GC) estimate as a normalized correlation between multiple data sequences [4]–[8]. However, the performance of a GC-based detector decreases when used with low signal-to-noise ratio[1] (SNR) data. This decrease may be counteracted by the addition of extra sensors to the GC-based detector system, but improvement requires the SNR of every newly added sensor to be at least 6 dB greater than the lowest SNR sensor in the system [8]. Also, while significant performance gains can be achieved with the addition of extra sensors, sensor cost may be a limiting factor. Hence, if one could obtain a relatively high SNR on one of the sensors, then an estimate of the signal, that can be substituted for the actual sensor data in the GC estimate with the other, lower SNR sensor measurements, is expected to provide improved performance [9]–[11].

In this paper, we propose the use of time-frequency based techniques as preprocessing tools to estimate the time-varying signal of interest from a high SNR sensor for use in the GC estimate. Specifically, we estimate signals with nonlinear phase functions using a modified version of the matching pursuit decomposition (MMPD) algorithm. The MMPD uses a dictionary with elements similar in time-frequency structure to the analysis signal. We also consider signal estimation by estimating the amplitude and instantaneous frequency (IF) of the signal based on a localized time-frequency representation (TFR) of the signal. We will demonstrate that, not only do such preprocessing steps yield detection performance improvement gains but they can also provide information that a GC-based only detector would require extra processing steps to determine.

This paper is organized as follows. In Section II, we provide an overview of the GC estimate approach for multisensor signal detection. We review the MMPD and IF estimation techniques in Section III. In Section IV, we propose the use of these signal estimation techniques to improve the detection performance of the GC estimate. In Section V, we provide a two-sensor example where we demonstrate the improved performance of the GC estimate when it employs a signal estimate from a high SNR sensor. We also compare the MSC estimate performance to a generalized likelihood ratio test statistic, and we investigate the effect of the two different estimates.

II. GC Estimate Multisensor Detection

The GC estimate provides a successful methodology for detecting a common but unknown signal on several spatially distributed sensors as it forms a statistic for measuring the similarity between two or more data sequences [4]–[8]. The GC estimate is an extension of the well-known MSC estimate

Manuscript received October 14, 2003; revised October 10, 2005. The associate editor coordinating the review of this manuscript and approving it for publication was Dr. Constantinos B. Papadias.

The authors are with the Department of Electrical Engineering, Arizona State University, Tempe, AZ 85287-7206 USA (e-mail: papandreou@asu.edu; cochran@asu.edu).

Digital Object Identifier 10.1109/TSP.2006.879284

[1]Throughout this paper, noise is assumed to be stationary, Gaussian, additive, and independent on each sensor channel. SNR is defined as the ratio of signal energy to noise variance.

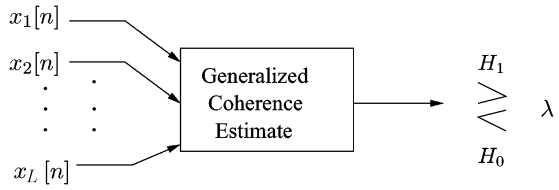

Fig. 1. Block diagram of the multisensor GC detector.

for two data sequences [1]–[3], and, as a result, it embodies many of the desirable properties of the MSC estimate [5]. An L-channel MSC-based detector is depicted schematically in Fig. 1. We consider the two-hypothesis scenario[2]

$$H_0: \quad x_l[n] = w_l[n] \tag{1}$$
$$H_1: \quad x_l[n] = s[n] + w_l[n] \tag{2}$$

for $l = 1, \ldots L$ and $n = 0, \ldots N-1$. Here, $s[n]$ corresponds to the common signal on the L sensors, $w_l[n]$ is complex, independent additive white Gaussian noise (AWGN) on the lth sensor, and $x_l[n]$ is the data observation from the lth sensor. Based on this scenario, the GC estimate statistic is given as [4]–[8]

$$\gamma^2_{L,N}(x_1, \ldots, x_L) = 1 - \frac{g(x_1, \ldots, x_L)}{||x_1||^2 \ldots ||x_L||^2} \tag{3}$$

where $g(x_1, \ldots, x_L)$ is the determinant of the Gram matrix

$$\mathbf{G}(x_1, \ldots, x_L) = \begin{bmatrix} \langle x_1, x_1 \rangle & \ldots & \langle x_1, x_L \rangle \\ \vdots & \ddots & \vdots \\ \langle x_L, x_1 \rangle & \ldots & \langle x_L, x_L \rangle \end{bmatrix}.$$

Here, the inner product is defined in discrete time as $\langle x, y \rangle = \sum_{n=0}^{N-1} x[n]y^*[n]$ and $||x||^2 = \langle x, x \rangle$. For $L = 2$ sensors, the MSC estimate statistic in (3) simplifies to

$$\gamma^2_{2,N}(x_1, x_2) = \gamma^2 = \frac{|\langle x_1, x_2 \rangle|^2}{||x_1||^2 ||x_2||^2}. \tag{4}$$

The probability distribution function of the MSC estimate is given by [1], [5]

$$Pr\{\gamma^2 \leq \lambda\} = 1 - (1-\lambda)^{N-1}, \quad 0 \leq \lambda \leq 1 \tag{5}$$

where λ is the detection threshold.

The statistical properties of the MSC and GC estimates are well understood for the H_0 hypothesis [4]–[8]. As a result, the probability of false alarm P_{FA} can be calculated from the H_0 hypothesis, and its corresponding probability of detection P_D can be obtained via Monte Carlo simulations. Derivations in [8] show that the P_{FA} of an MSC estimate $(L = 2)$ is

$$P_{\mathrm{FA}} = Pr\left(\{\gamma^2 > \lambda\}\right) = (1-\lambda)^{N-1}. \tag{6}$$

Thus, for a fixed P_{FA}, the detection threshold is $\lambda = 1 - (P_{\mathrm{FA}})^{1/(N-1)}$. As the number of sensors increases, new expressions for the P_{FA} and the corresponding thresholds can be obtained as shown in [5]. For example, for $L = 3$ sensors, it can be shown that

$$P_{\mathrm{FA}} = (1-\lambda)^{N-1} + (N-1)(N-2)(1-\lambda)^{N-1} \times \log(1-\lambda) + (N-1)^2 \left[(1-\lambda)^{N-2} - (1-\lambda)^{N-1}\right].$$

The P_{FA} for higher order multisensor detectors can be calculated using similar techniques as in the two- and three-sensor detection cases. Specifically, a recursion formula was obtained in [5] for the distribution of the GC estimate for larger number of sensors. The GC estimate was shown to yield remarkable results for moderate noise levels, but its performance deteriorates as the data sequences become very noisy [8]. Work in [5] showed that the addition of an extra sensor to the GC-based detector system (increasing L) improves the detector performance provided the SNR of the newly added sensor is at least 6 dB higher than the poorest sensor in the original system. In this paper, we propose the use of time-frequency methodologies to improve the performance of the GC estimate even at low SNRs when a time-varying signal is received from multiple sensors.

III. Time-Frequency Methodologies for Signal Estimation

Time-varying signals are signals whose spectral content varies with time. Examples of such signals include the generalized chirp

$$x(t) = e^{j2\pi\beta\eta(t/t_r)} \tag{7}$$

that has nonlinear phase function $\eta(t/t_r)$. Here, t_r is a positive reference time point (which we set to unity in the rest of the paper without loss of generality) and β is the signal's frequency-modulation (FM) rate. The signal's IF is given by the derivative of the phase function $\xi(t) = \beta \frac{d}{dt}\eta(t/t_r)$ and describes the frequency variation of the signal as a function of time. Due to this variation, classical Fourier-based techniques are not adequate for processing such signals. Instead, TFRs or time-frequency-based techniques can jointly provide a signal's time-frequency information [12]–[14].

Our goal is to use time-frequency techniques to obtain a noise-suppressed estimate of the highest SNR sensor output in a multisensor detector of time-varying generalized chirp signals. The time-frequency techniques include a modified matching pursuit decomposition iterative algorithm and IF estimation techniques from TFRs. The output estimate can then be used as part of the GC estimate to increase the detection performance of the common signal on the other, lower SNR, sensors.

A. Modified Matching Pursuit Decomposition Approach

The matching pursuit algorithm was proposed by Mallat [15] to decompose any signal into a linear expansion of waveforms that belong to a redundant dictionary. The elements of this dictionary consist of time-frequency shifted and scaled versions of one basic atom that is chosen to be a Gaussian signal due to its high localization in the time-frequency plane. The atoms are also allowed to rotate in the time-frequency plane in [16]. Although this is an iterative nonlinear algorithm, it can preserve signal energy

[2]Throughout this paper, we interchangeably refer to both continuous-time signals $x(t)$ and their appropriately sampled versions $x[n] = x(nT)$, where T is the sampling period.

due to its use of orthogonal expansions and can guarantee convergence [15]. As a result, it has been used in many applications including analysis and classification [17]–[22]. Depending on the time-frequency structure of the analysis signal, the matching pursuit algorithm may require many dictionary elements to decompose it, and thus can become very computationally intensive. In order to process signals with different types of time-frequency characteristics, a modified version of the matching pursuit decomposition algorithm expands the analysis signal into dictionary waveforms that match it in time-frequency structure [23], [24]. The advantage of using a dictionary matched to the analysis data is that only a small number of elements is used to decompose a signal, and thus fewer iterations are required, leading to a parsimonious representation.

B. IF Estimation Approach

The IF is a representation that ideally depicts the time varying spectral peaks of only monocomponent signals. In general, when the signal is multicomponent [such as a linear combination of signals of the form in (7)], then the IF does not provide an accurate representation. Various methods have been proposed in the literature to estimate IF based on TFRs including (but not limited to) [25]–[37]. This is because the IF of a signal follows the highly localized region of a TFR, and a mapping of this region can yield the IF estimate [28]. This entails that the chosen TFR can provide a highly concentrated signal representation.

Different TFRs are best suited for different signal structures [14], and the ideal choice of TFR for IF estimation is the one that produces the best time-frequency localization for the signal under consideration. For example, the Wigner distribution (WD) or Cohen's class TFRs [12], [38] are best suited for signals with linear structures in the time-frequency plane such as sinusoids or linear FM chirps. On the other hand, hyperbolic chirps (signals with hyperbolic IF) are best analyzed using the Altes Q-distribution or other hyperbolic class TFRs [39], [40].

IV. GC-Based Detection With Signal Estimation

In many multisensor signal-processing applications, one of the sensors will have a relatively higher SNR than all the other sensors in the system. Note that this sensor is often known in practice. For example, in passive sonar applications, the signal of interest is often initially detected on a single-channel basis, but time difference of arrival estimation with other sensors is highly desirable for geographic localization of the signal source. However, the signal is often considerably weaker on other sensors due to distance from the source or acoustic convergence zone effects. If not known in advance, the sensor with the maximum SNR can be found by estimating the noise variance [41] and then choosing the sensor with the lowest noise variance estimate. Our multisensor detection method proposes to extract the common signal from the highest SNR sensor using either the MMPD algorithm or the IF estimation method. The extracted signal will then be used to detect the presence of the signal from the remaining low SNR sensors. Note that for the hypothesis testing of the GC-based detection system to be valid, we assume that the signal $s[n]$ in (2) to be extracted is a time-varying generalized chirp in (7) that is identical on all the L sensors.

A. MMPD and GC-Based Detection

1) MMPD Approach: For the MMPD approach, we form a dictionary using waveforms that are matched, in time-frequency structure, to the signals of interest; in our case, these signals correspond to the time-varying generalized chirps in (7). For example, in a sonar multisensor detection application, a linear FM chirp could be chosen to form the dictionary; this signal has quadratic phase $\eta(t) = t^2/2$ and linear IF $\xi(t) = \beta t$ in (7). In order for the dictionary to be complete, we transform the basic signal atom via time-frequency shifts as well as a transformation that causes a constant shift to the IF of the waveform [23], [24]. In the case of linear FM chirps, this corresponds to a constant shift in the FM rate; that is, if $x(t) = e^{j2\pi\beta_0 t^2/2}$ is a linear FM chirp with rate β_0, then the aforementioned transformation yields $e^{-j2\pi\beta_1 t^2/2}x(t) = e^{j2\pi(\beta_0-\beta_1)t^2/2}$ which is another linear FM chirp with rate $(\beta_0-\beta_1)$. In the time-frequency plane, this corresponds to a change in the slope of the linear instantaneous frequency of the chirp. Thus, if the basic signal atom is the time-varying generalized chirp $g(t) = e^{j2\pi\eta(t)}$ [the signal in (7) with $\beta = 1$], then the dictionary elements are formed as

$$g(t;\tau,\nu,\beta) = g(t-\tau)e^{-j2\pi\nu t}e^{-j2\pi\beta\eta(t)} \tag{8}$$

for different ranges of the time shifts τ, frequency shifts ν, and IF shifts β. The specific ranges of these transformation parameters depend on the application at hand, and, if possible, they should be limited to reduce the size of the dictionary and thus the MMPD algorithm computational complexity. Note that the dictionary can be composed of more than one basic atom of the form in (8) with different phase functions $\eta(t)$. To create the dictionary for such a case, we can allow each basic atom to undergo its corresponding transformation in (8) by changing $\eta(t)$ accordingly.

Following the original matching pursuit algorithm [15] and the MMPD algorithm [24], a given signal $x(t)$ that is to be decomposed using the MMPD is first correlated with every element in the dictionary, and the dictionary element that provides the maximum correlation is denoted as $g(t;\tau_1,\nu_1,\beta_1)$. This selected atom is the waveform that is most similar to the analysis signal $x(t)$. Specifically, during the first iteration

$$x(t) = \left(R^{(1)}x\right)(t) = \alpha_1 g(t;\tau_1,\nu_1,\beta_1) + \left(R^{(2)}x\right)(t) \tag{9}$$

where $\alpha_1 = \langle (R^{(1)}x)(t), g(t;\tau_1,\nu_1,\beta_1)\rangle = \int (R^{(1)}x)(t)g^*(t;\tau_1,\nu_1,\beta_1)dt$. The residue $(R^{(2)}x)(t)$ is obtained by subtracting from $x(t)$ the first expansion element $g(t;\tau_1,\nu_1,\beta_1)$ that is weighted by the correlation coefficient α_1 [(see (9)]. Since $(R^{(2)}x)(t)$ can be shown to be orthogonal to $g(t;\tau_1,\nu_1,\beta_1)$, then it can be shown that

$$\|x\|^2 = |\langle x(t), g(t;\tau_1,\nu_1,\beta_1)\rangle|^2 + \left\|R^{(2)}x\right\|^2.$$

Note that $\|R^{(2)}x\|$ is minimized by choosing $g(t;\tau_1,\nu_1,\beta_1)$ such that $|\alpha_1|$ is maximum. The residue is iteratively subdecomposed such that at the kth iteration, it is given by

$$\left(R^{(k)}x\right)(t) = \alpha_k g(t;\tau_k,\nu_k,\beta_k) + \left(R^{(k+1)}x\right)(t)$$

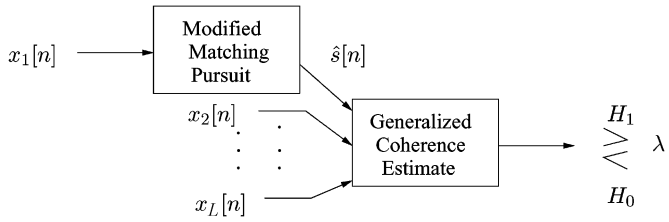

Fig. 2. Block diagram of a GC detector that utilizes MMPD estimation.

where $\alpha_k = \langle (R^{(k)}x)(t), g(t;\tau_k,\nu_k,\beta_k)\rangle$. Ideally, this decomposition continues until the residue $(R^{(k)}x)(t)$ becomes zero. In practice, if $x(t)$ is decomposed K times, then it can be approximated as

$$x(t) = \sum_{k=1}^{K} a_k g(t;\tau_k,\nu_k,\beta_k). \tag{10}$$

It should be noted that the MMPD forms its dictionary such that K is small for any signal decomposition [24]. A monocomponent linear FM chirp, for example, could be decomposed with a single iteration if the chirp is a member of the dictionary. For any received signal $x(t)$ of appreciable SNR, signal components are more localized than noise components and will have the highest correlation with matched dictionary atoms. The MMPD uses this property to extract signal atoms until some iteration K when nearly all signal atoms have been extracted or when the residual signal energy is less than a fixed threshold. The MMPD results in a small mean square error (MSE) provided that the number of iterations or the energy threshold are chosen such that very little noise enters the estimate in (10). This can be achieved by first preprocessing the signal to be decomposed in order to estimate the number of signal components and thus limit the number of iterations accordingly. The preprocessing can also be used to determine the time-frequency structure of the signal if it is not known a priori, as this information is necessary to correctly form the dictionary. Another method to ensure low MSE using the MMPD is to increase the fineness of the dictionary grid; this, however, will increase computational complexity. Note that more details on the MMPD algorithm can be found in [24].

2) GC-Based Detection: The block diagram of the MMPD approach with the GC estimate is given in Fig. 2. Here, we assume that the observation $x_1[n]$ from Sensor 1 has high SNR, and it will be used to obtain a signal estimate $\hat{s}[n]$ in (2). In order to demonstrate the successful performance of the MMPD method in extracting a noise-free signal from a high SNR signal, we consider a linear FM chirp signal in noise with SNR $=-3$ dB. Recall that the IF of such a signal is a line in the time-frequency plane, as is demonstrated by the highly localized WD TFR in Fig. 3. The WD of the high SNR chirp is plotted in Fig. 3(a), and the WD of the corresponding decomposed signal using the MMPD is shown in Fig. 3(b). Fig. 3(c) shows the WD of a -19 dB SNR signal from the second, low SNR sensor to be detected using the proposed method. Note that the signal would be difficult to detect simply from the Sensor 2 measurement. The GC estimate performance is expected to be higher when the noise-free extracted signal in Fig. 3(b) is used instead of the high SNR signal in Fig. 3(a).

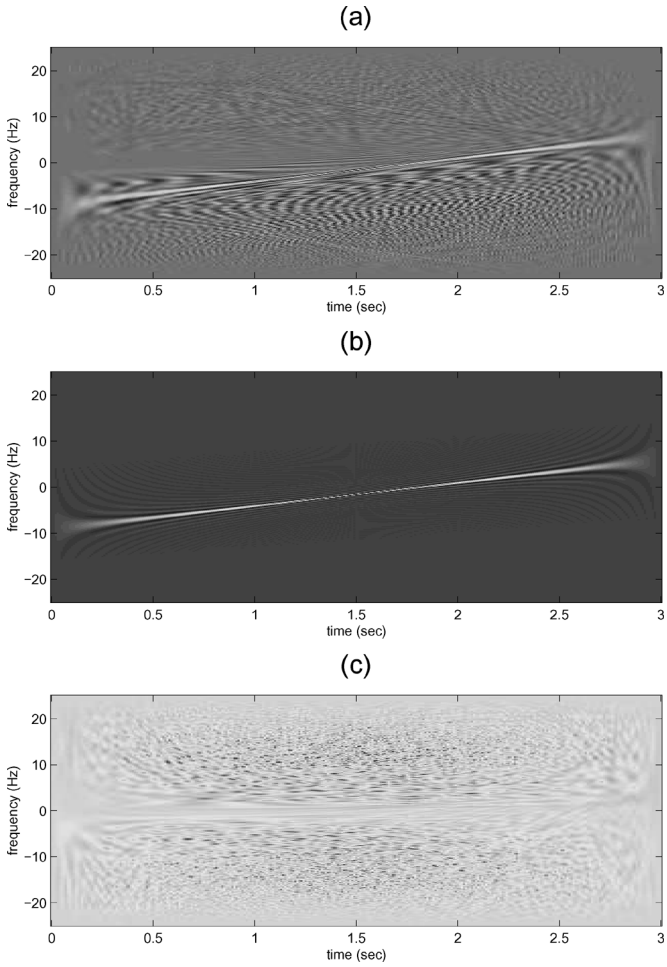

Fig. 3. WD of (a) Sensor 1 output with SNR $=-3$ dB, (b) MMPD output of Sensor 1, and (c) Sensor 2 output with SNR $=-19$ dB.

B. IF Estimation and GC-Based Detection

1) IF Estimation: Although with a matched dictionary the decomposition can be parsimonious, the MMPD may still have high memory usage and can be computationally intensive. Another time-frequency technique capable of generating a noise-suppressed equivalent of the high SNR sensor, but with lower computational and memory requirements than the MMPD, is the use of time-frequency-based IF estimation techniques.

When the signals are linear FM chirps, then we use the WD[3] for estimating their linear IF $\xi(t) = \beta t$ in (7). The WD of a signal $x(t)$ is defined as

$$\mathrm{WD}_x(t,f) = \int_{-\infty}^{\infty} x(t+\tau/2)x^*(t-\tau/2)e^{-j2\pi f\tau}d\tau.$$

Indeed, the WD of a linear FM chirp $x(t) = e^{j2\pi\beta t^2/2}$ can be obtained in closed form as the highly localized representation

[3]In practice, the signals in (7) would correspond to the analytic signal representations of the real data obtained from the sensors, and the Wigner–Ville distribution would be used instead of the Wigner distribution [25].

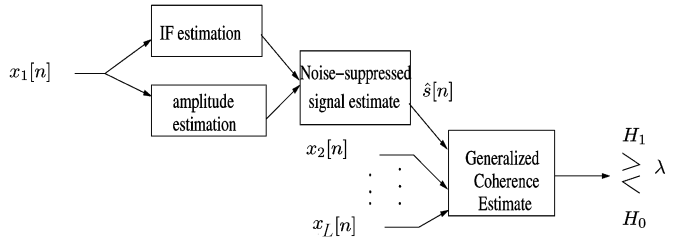

Fig. 4. Block diagram of a GC detector that utilizes time-frequency IF estimates. Here, $x_1[n]$ is assumed to be the output of the highest SNR sensor and $\hat{s}[n]$ is the noise-suppressed signal estimate.

$\mathrm{WD}_x(t,f) = \delta(f - \beta t)$. This corresponds to a line in the time-frequency plane, which is the IF of the chirp, whose slope is the FM rate β. Thus, using the WD, the estimate $\hat{\xi}(t)$ of the linear IF can be obtained as [10], [28]

$$\hat{\xi}(t) = \arg\left\{\max_f \left[\mathrm{WD}_x(t,f)\right]\right\}. \tag{11}$$

Note that, as the data have finite duration in practice, the variance of the IF estimate in (11) will increase due to time-windowing effects in the WD computation.

When the signals are multicomponent linear FM chirps, the WD may not be the most suitable IF estimation approach, as it contains oscillatory cross terms. For these signals, other smoothed TFRs of Cohen's class may be more appropriate for use in the estimation.

When the signals are nonlinear FM chirps [the generalized chirp in (7) with an arbitrary nonlinear IF $\xi(t)$], then we use the matched warped Wigner distribution (WWD). For a signal $x(t)$, the WWD with warping function $\zeta(t)$ is given by [42]

$$\mathrm{WWD}_x(t,f) = \mathrm{WD}_{\mathcal{W}x}\left(t_r\rho(t/t_r), \frac{f}{t_r\zeta(t)}\right) \tag{12}$$

where $(\mathcal{W}x)(t) = |t_r\zeta(\rho^{-1}(t/t_r))|^{-1/2}x(t_r\rho^{-1}(t/t_r))$ is the warped signal, $\zeta(t) = \frac{d}{dt}\rho(t/t_r)$, and $\rho^{-1}(\rho(t/t_r)) = t/t_r$ is the inverse function. It can be shown that the WWD in (12) of the signal in (7) is highly localized along the signal's matched nonlinear IF $\xi(t)$ [42] provided that $\eta(t/t_r) = \rho(t/t_r)$. Thus, the estimate of the nonlinear IF can be obtained as in (11) but with the WD replaced by the WWD in (12).

2) GC-Based Detection: Assuming a constant amplitude A for the signal $x(t)$ in (7), if one could obtain very good estimates of the signal's amplitude $\hat{A}$ and IF $\hat{\xi}(t)$, then a noise-suppressed estimate of the signal can be reconstructed from these estimates as $\hat{s}(t) = \hat{A}e^{j2\pi\int\hat{\xi}(t)dt}$. Thus, this signal estimate could be used as part of the GC-based detection, instead of the MMPD estimate, to reduce the computational cost of the MMPD and still yield improved detector performance. Fig. 4 depicts a block diagram of this approach. The amplitude estimate can be obtained using maximum likelihood techniques [41] once the IF is estimated from a TFR. Note that the signal estimate $\hat{s}[n]$ from Sensor 1 in Fig. 4 depends on the estimates $\hat{A}$ and $\hat{\xi}(t)$. Hence, any bias in the IF estimates will have a significant effect on the detector performance. The examples we consider in this paper estimate single linear FM chirps using the WD. As a result, a peak detector is employed to locate the peak of the WD for all time instants, corresponding to the linear IF of the chirp in the time-frequency plane. Poor localization of noise components in the time-frequency plane enables this method to work well, but performance deteriorates as the noise components become stronger.

V. Simulations and Performance Comparisons

In order to demonstrate the performance of our proposed methods, we simulate a two-sensor detection problem with a complex linear FM chirp sequence of length $N = 300$ in complex zero-mean AWGN of known variance σ^2, and for varying SNRs. Although we considered a single component, the simulations could be similarly extended to multicomponent signals. We first consider an MSC-based detector that uses the Sensor 1 decomposed signal from a) the MMPD algorithm (MSC-MMPD) and b) the IF estimation technique (MSC-IF). We compare the performance of the MSC estimate (used without prior signal estimation) with the MSC estimate that uses an estimate of the common signal from the highest SNR sensor.

For further comparison, we also consider a generalized likelihood ratio test (GLRT) statistic [41] for the two-sensor problem with both the MMPD (GLRT-MMPD) and the IF (GLRT-IF) estimation techniques. A GLRT-based detector pertains to the detection problem of a deterministic signal with unknown parameters in AWGN [41]. Here, the MMPD will be used to obtain a reasonably good estimate of the transmitted signal from the high SNR sensor permitting the use of a GLRT statistic. The MMPD decomposed signal estimate has a low MSE [9], [10]. Thus, the resulting GLRT-MMPD detector (though not optimal) is expected to be close to the optimal matched filter (that assumes full knowledge of the signal) detector performance depending on the MSE of the MMPD.

All methods are simulated using 1000 Monte Carlo simulations, and the results are demonstrated using receiver operating characteristic (ROC) curves of probability of detection P_D versus probability of false alarm P_{FA}. For all our figures, the worst performance, which is obtained for the lowest SNR on Sensor 1, is depicted by the rightmost curve for any of the methods. For the MSC estimate, the P_{FA} is obtained from (6), whereas the P_D is obtained from the Monte Carlo simulations. The GLRT detection statistic for the output of a noisy sensor is derived in [41] as

$$T(x) = \sum_{n=0}^{N-1} x[n]\hat{s}^*[n] - \frac{1}{2}\mathcal{E}_{\hat{s}}$$

where $\mathcal{E}_{\hat{s}}$ is the energy of the estimated signal $\hat{s}[n]$. The P_{FA} for a detection threshold λ is given by

$$P_{\mathrm{FA}} = Q(\lambda/\sqrt{\sigma^2\mathcal{E}_{\hat{s}}/N})$$

where $Q(x) = \int_x^\infty (1/\sqrt{2\pi})e^{-t^2/2}dt$ is the Q-function [41]. Note that the GLRT approach can be depicted as in Figs. 2 and 4 but with the GC estimate replaced by the GLRT statistic.

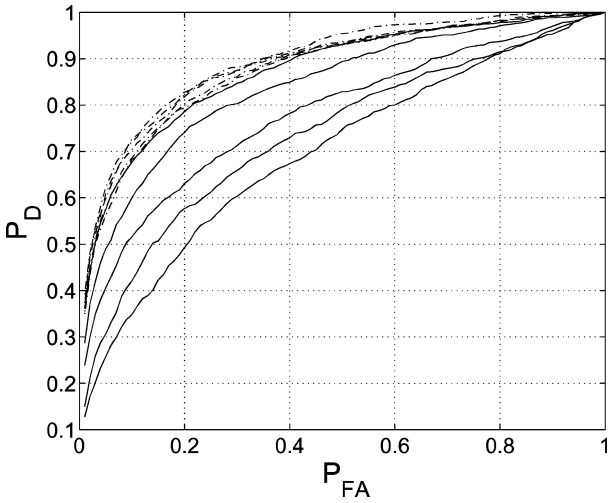

Fig. 5. ROC curves showing the stable performance of the MSC-MMPD (cluster of dash-dotted lines) to the diminishing performance of the MSC-based detector (solid lines) as Sensor 1 SNR decreases from 10 dB to −10 dB (in 5 dB steps), with a fixed −19 dB SNR on Sensor 2.

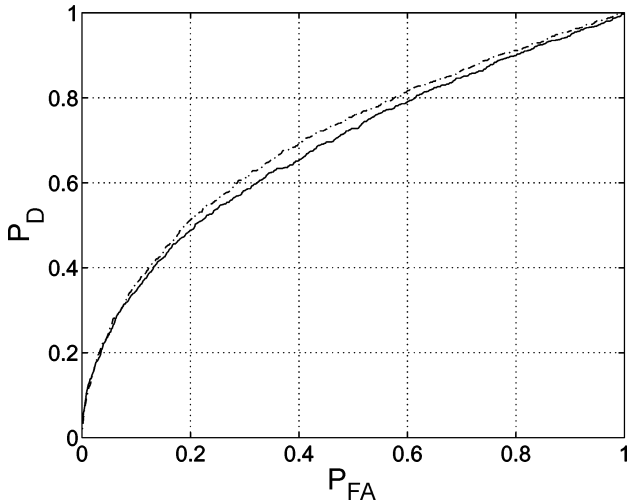

Fig. 6. ROC curves for MSC estimate (solid line) and MSC-MMPD detector performances for 0 dB SNR on Sensor 1 and very low SNR (−25 dB) on Sensor 2.

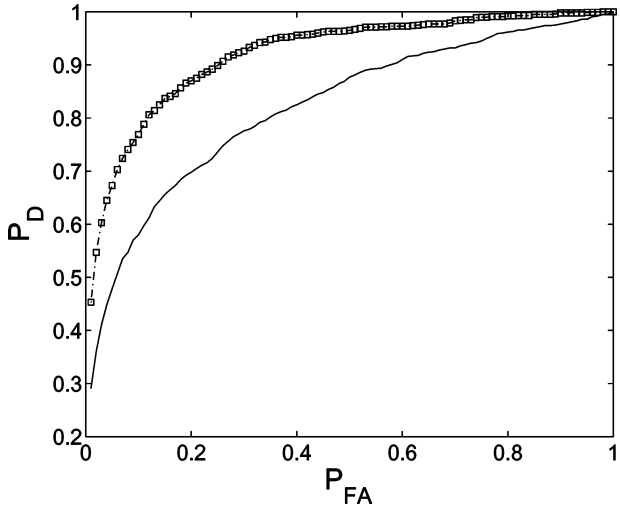

Fig. 7. ROC curves demonstrating the negligible effect of underdecomposing Sensor 1 if the undecomposed components are small in magnitude. Shown here are an MSC-based detector (solid line), an MSC-MMPD that used the fully decomposed Sensor 1 data (squares), and an MSC-MMPD that used the underdecomposed Sensor 1 data (dash-dotted line). Here, the SNR is 0 dB on Sensor 1 and −19 dB on Sensor 2.

A. MMPD Estimation and MSC-Based Detection

Fig. 5 shows the performance of the MSC-MMPD (dash-dotted lines) compared to the MSC-based detector (solid lines) for a fixed −19 dB SNR on Sensor 2, while the Sensor 1 SNR decreases from 10 dB to −10 dB (in steps of 5 dB). This ascertains that the MSC estimate performs well for high Sensor 1 SNRs, but its performance retrogresses as Sensor 1 becomes noisier. Our proposed preprocessing method retains high performance even for low Sensor 1 SNRs (as seen by the closeness of the MSC-MMPD ROC curves in Fig. 5). This is because the MMPD estimate is quite accurate even at low SNRs. Note that both methods produce comparably good performance when Sensor 1 has high SNR (10 dB). This is because we expect that the estimate obtained from the MMPD approximately equals the original Sensor 1 output if Sensor 1 has high SNR. As no preprocessing was performed on Sensor 2, any increase (or decrease) in Sensor 2 SNR will have similar performance gains (or losses) in both the MSC-based and MSC-MMPD detectors. However, for a very low SNR on Sensor 2, the common signal will be overwhelmed by noise and no amount of preprocessing on the output of Sensor 1 will yield any performance gain as demonstrated in Fig. 6.

Ideally, the MMPD should be terminated after all signal terms have been extracted or when noise terms become the most localized terms in the TFR of the residual signal [15], [24]. If the MMPD is terminated long before this critical point (i.e., underdecomposed), then if the residual terms are low in energy, it is possible that the effect on the performance is minimal. This is demonstrated in Fig. 7 where the signal consists of three linear FM chirps, but two of these chirps have very low amplitudes. On the other hand, if these two terms are dominant in the transmitted signal, then they will be lost and hence a larger MSE for the noise-suppressed estimate (and consequently poorer performance gain) will be obtained. This is demonstrated in Fig. 8. Similarly, if the MMPD is continued even after this critical point (i.e., overdecomposed), noise terms will be included in the noise-suppressed estimate resulting in poor detection performance. Additional performance plots investigating these cases can be found in [11].

B. MMPD Estimation and GLRT-Based Detection

Fig. 9 shows the performance of the GLRT-MMPD (dash-dash lines) compared to the MSC-based detector (solid lines) for a fixed −19 dB SNR on Sensor 2, while the Sensor 1 SNR decreases from 10 dB to −10 dB (in steps of 5 dB). The scenario is similar to the one in Fig. 5 with an MSC-MMPD. When we compare these two figures, we observe improved detector performances of the GLRT-MMPD over the MSC-MMPD. While negligible performance gains are obtained with the MSC-MMPD for high Sensor 1 SNRs (see Fig. 5), we observe significant gains with the GLRT-MMPD. So, even for high SNRs on Sensor 1, the GLRT-MMPD yields significant perfor-

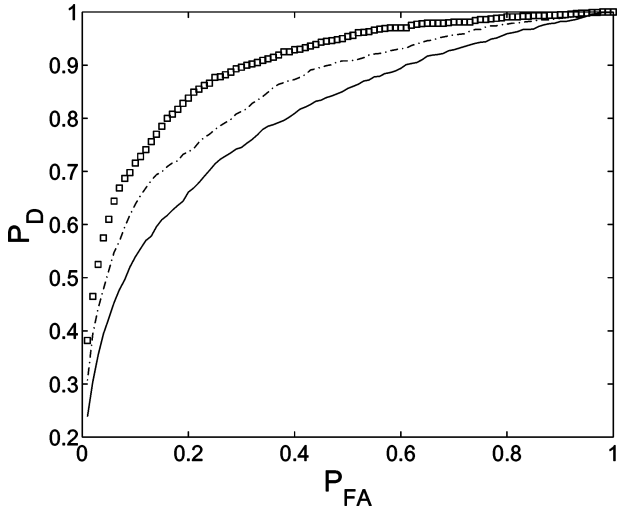

Fig. 8. ROC curves demonstrating the adverse effect of underdecomposing Sensor 1 if the undecomposed components are dominant terms. Shown here are an MSC-MMPD detector that used the fully decomposed Sensor 1 data (squares), an MSC-MMPD detector that used an underdecomposed Sensor 1 data (dash-dotted) and an MSC-based detector (solid line). Here, the SNR is 0 dB on Sensor 1 and −19 dB on Sensor 2.

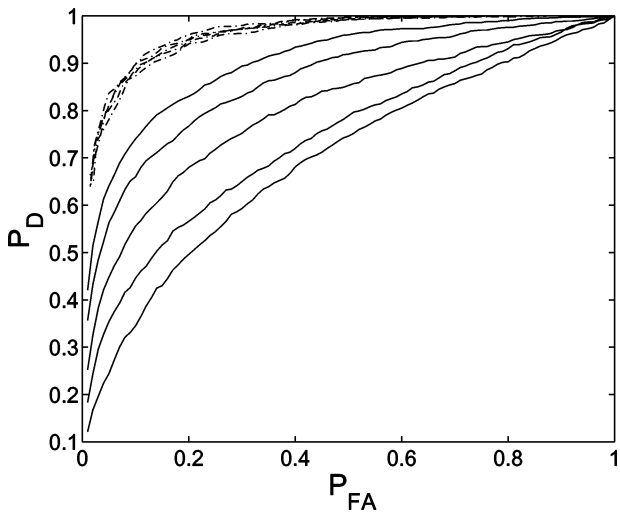

Fig. 9. ROC curves comparing the stable performance of the GLRT-MMPD (cluster of dash-dash lines) to the diminishing performance of the MSC-based detector (solid lines) as the SNR of Sensor 1 decreases from 10 dB to −10 dB (in 5 dB steps) for a fixed −19 dB SNR on Sensor 2.

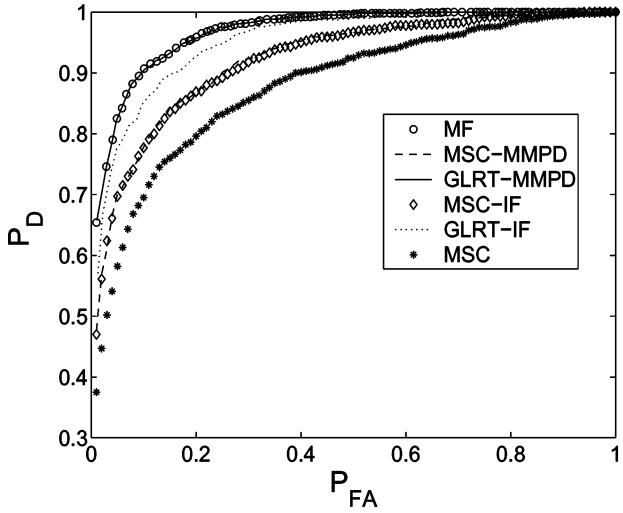

Fig. 10. ROC curves for five detectors for 5 dB SNR on Sensor 1 and −19 dB SNR on Sensor 2. The detectors are the MSC-based (no signal estimation), matched filter (MF) (assuming full signal knowledge), MSC-MMPD, MSC-IF, GLRT-MMPD, and GLRT-IF.

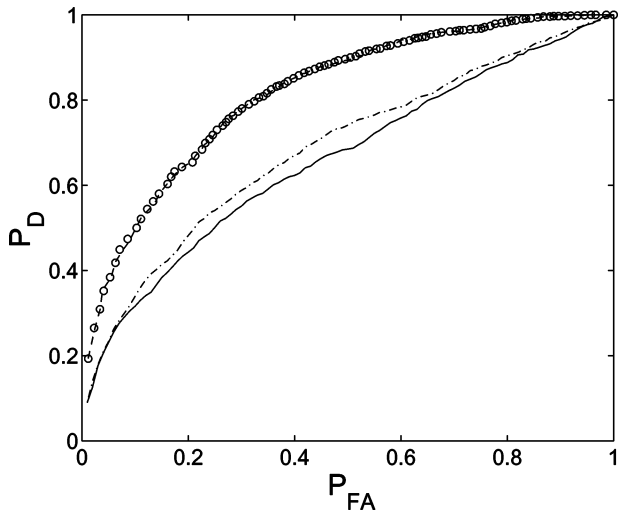

Fig. 11. ROC curves demonstrating the performance gain of the GLRT-MMPD detector even for very low SNRs on Sensor 2. Shown here are the performance of the optimal matched filter (MF) detector (circles) and MSC-based detector (solid line), compared to a GLRT-MMPD detector (dash-dash) and an MSC-MMPD detector (dash-dotted) for −10 dB SNR on Sensor 1 and −25 dB on Sensor 2.

mance gains over the MSC estimate, unlike the MSC-MMPD that resulted in similar performance as the MSC estimate. As the noise-suppressed MMPD estimate obtained from the high SNR sensor has a very small MSE, the resulting performance of the GLRT-MMPD is comparable to that of an optimal matched filter, where the signal is assumed completely known. Fig. 10 shows the performance of a GLRT-MMPD (solid line) to be approximately the same as an optimal matched filter (circles) as they overlap each other. This simulation used 5 dB SNR on Sensor 1 and −19 dB SNR on Sensor 2.

Except for the increase in gain, the performance pattern of the GLRT-MMPD follows that of the MSC-MMPD (see Figs. 5 and 9). Note that with the near optimal performance, the GLRT-MMPD also permits reasonable detection even at lower Sensor 2 SNRs; on the other hand, the MSC and MSC-MMPD methods succumb to the poorer detector performance associated with lower SNRs as demonstrated in Fig. 11. Note that, similarly to the MSC-MMPD, the GLRT-MMPD performance deteriorates as the MSE of the MMPD estimate increases.

C. IF Estimation and MSC-Based Detection

The IF estimation technique was shown to be a viable alternative for the MMPD algorithm due to its reduced computational complexity. However, it yielded favorable MSEs only for a limited range of SNRs. This is attributed to the tradeoff between performance and computational cost for signal estimates. Fig. 12 compares the performance of the MSC-IF to the MSC estimate over the range of Sensor 1 SNRs considered for

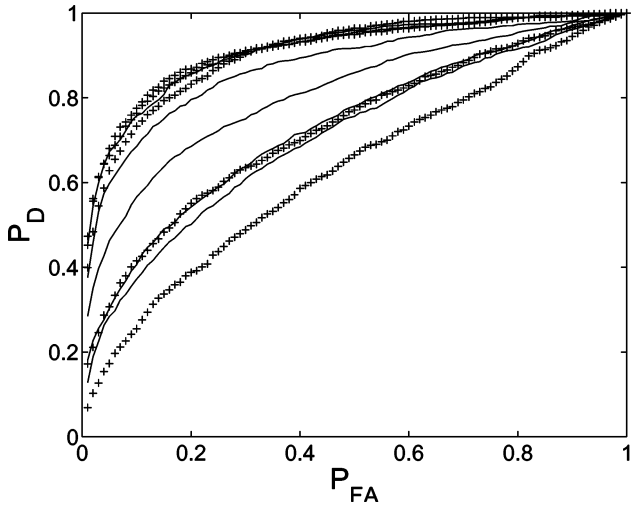

Fig. 12. ROC curves comparing the MSC estimate (solid lines) to the MSC-IF as the SNR of Sensor 1 decreases from 10 dB to −10 dB (in 5 dB steps). Sensor 2 SNR is −19 dB.

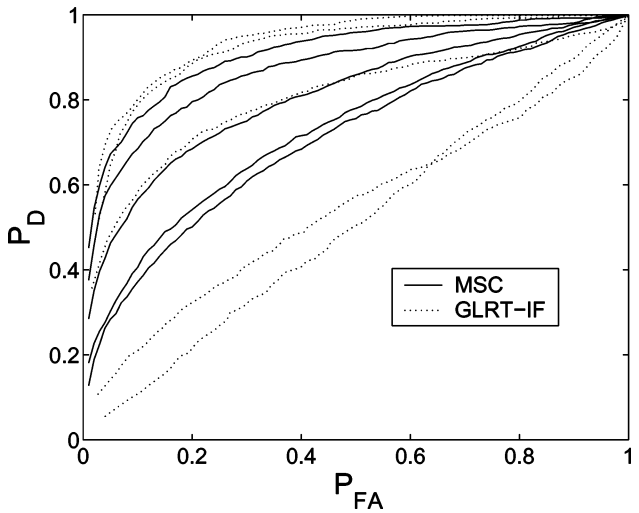

Fig. 13. ROC curves comparing the MSC estimate (solid lines) to the GLRT-IF (dotted lines) as the SNR of Sensor 1 decreases from 10 dB to −10 dB (in 5 dB steps). Sensor 2 SNR is −19 dB.

the MSC-MMPD. The MSC-IF outperforms the MSC-based detector for high Sensor 1 SNRs, but it is more susceptible to noise than the MSC-MMPD in Fig. 5. The favorable region of operation for the MSC-IF is between −5 and 10 dB, compared to the −12 dB (not shown in Fig. 5) and 10 dB of the MSC-MMPD. However, within this favorable region, the MSC-IF in Fig. 12 performs comparably to the MSC-MMPD in Fig. 5.

D. IF Estimation and GLRT-Based Detection

Fig. 13 summarizes the performance of the GLRT-IF over the range of Sensor 1 SNRs considered for the preceding methods. The GLRT-IF outperforms the MSC-based detector (solid lines) for high SNRs but has the narrowest range of Sensor 1 SNRs (0 to 10 dB) for improved performance gain. Because of that, the magnitude of the performance gain for the GLRT-IF (outside its favorable region of operation) is the least among all the proposed methods. This is because the GLRT statistic requires a low MSE signal estimate, compared to the higher signal MSE obtained via IF estimation. Note that the GLRT-IF has lower performance that the GLRT-MMPD in Fig. 10. When Sensor 1 has 5 dB SNR as in Fig. 10, as the GLRT-IF is within its favorable region of operation, it still outperforms both the MSC and the MSC-MMPD methods.

E. Discussion

Based on our simulation comparisons for the two-sensor detection problem, we can make some deductions regarding the two detection statistics—the MSC and the GLRT—and the two signal estimation methods—the MMPD and the IF. Note that Fig. 10 provides a comparison between the four different combinations of detectors: MSC-MMPD, GLRT-MMPD, MSC-IF, and GLRT-IF. For a fair comparison, the SNR on Sensor 1 was chosen to be 5 dB in order to include a favorable region of operation that is common to all proposed methods.

- The MSC-MMPD provides improved performance over using the MSC that does not employ prior signal estimation. The performance deteriorates only when there is a very low SNR on one or all the sensors and when the MMPD signal estimate has a large MSE error. This large error could result either from an insufficient or an excessive number of iterations. Depending on the application, the computational intensity of the MMPD could be reduced by using a small dictionary as that would decrease the number of correlation operations needed per iteration. This could also be achieved by some initial processing to obtain information about the time-frequency structure of the signal or the number of its components.
- Since the estimate obtained from the MMPD has low MSE, the GLRT-MMPD has higher performance than the MSC-MMPD. This is because, depending on the MSE between the estimated and the true transmitted signal, the performance of the GLRT-MMPD can be comparable to the matched filter where the signal is assumed completely known. Thus, the tremendous improvement in detector performance (even at much lower Sensor 1 SNRs) of the GLRT-MMPD makes it very suitable for two-sensor detection in high noise applications when compared to the MSC-MMPD. The performance of the GLRT-MMPD, just like the MSC-MMPD, also highly depends on the resulting MSE from the MMPD algorithm.
- The MSC-IF or the GLRT-IF can be used instead of the MSC-MMPD or GLRT-MMPD when computational power and memory are limited. From Fig. 10, for a relatively high SNR on Sensor 1, the IF estimation approach will be chosen over the MMPD for a tradeoff between cost and performance.

Note that the GLRT approach has only been verified for the two-sensor problem; for multiple sensors, the GC estimate is applicable as discussed in Section II.

VI. Conclusion

The GC estimate provides a statistic for detecting the presence of a common signal on multiple sensors. It extends the widely used magnitude-squared coherence estimate approach for the two-sensor detection. However, the performance of the

GC-based detector diminishes significantly in high noise environments. To offset the degrading performance, the GC estimate would require the use of extra sensors with SNRs at least 6 dB greater than the worst sensor already in the system. In this paper, we proposed to estimate the signal from the sensor with the highest SNR in the multisensor detection of time-varying generalized chirp signals, and then use the estimate with the GC estimate to detect the presence of the signal on the other, even noisier, sensors for improved overall detection performance.

One of our proposed techniques uses the modified matching pursuit algorithm that is based on generating the dictionary from waveforms that match, in time-frequency structure, the signal to be estimated. The success of this method depends on knowing the signal structure of all signal components and an approximate number of the signal components. As this information is not always available for all applications, different time-frequency based techniques can be used to preprocess the signal and extract the necessary information a priori. This method can result in low MSE errors, and can thus provide a noise-free estimate to be used with the GC-based detector. As we have demonstrated, this method results in remarkable performance gains over simply using the GC estimate without signal estimation. As this is an iterative algorithm, it can be computationally intensive, especially when no a priori information is available on the signal. Without specific signal information, the original matching pursuit decomposition can be used with Gaussian waveforms as the basic atom in the dictionary, but the number of iterations needed may be large before convergence.

In order to reduce the computational complexity of the MMPD, we also proposed to estimate the time-varying signal using IF estimation techniques that are based on highly localized TFRs. With this method, the estimate was not as accurate, but in some applications trading a small level of performance for computational cost may be of essence. Note that recent studies in IF estimation may be used to improve the estimation accuracy.

As we showed, the GC estimate can be applied to a set of L sensors in applications such as source detection and localization. For the two-sensor problem, we also obtained a GLRT-based detector making use of the estimated signals from the high SNR sensor. With the GLRT statistic, we observed performance gains even for very low-SNR sensors, for which an MSC estimate, with or without the extracted signal, had poor performance. Overall, we have successfully showed via simulation that these time-frequency preprocessing techniques can be used to significantly improve the performance of a GC-based multisensor detector without having to increase the number of sensors in the GC estimate detection system.

ACKNOWLEDGMENT

The authors would like to thank the anonymous reviewers for valuable comments that led to improvements in this paper.

REFERENCES

[1] G. C. Carter, C. Knapp, and A. H. Nuttall, "Estimation of the magnitude-squared coherence function via overlapped fast Fourier transform processing," *IEEE Trans. Audio Electroacoust.*, vol. AE-21, pp. 337–344, Aug. 1973.

[2] R. Trueblood and D. Alspach, "Multiple coherence," in *Proc. 11th Asilomar Conf. Signals, Syst. Comput.*, Apr. 1977, pp. 327–332.

[3] H. Gish and D. Cochran, "Invariance of the magnitude squared coherence estimate with respect to second channel statistics," *IEEE Trans. Acoust., Speech, Signal Process.*, vol. ASSP-35, pp. 1774–1776, Dec. 1987.

[4] ——, "Generalized coherence," in *Proc. IEEE Int. Conf. Acoust., Speech Signal Process.*, April 1988, vol. 5, pp. 2745–2748.

[5] D. Cochran and H. Gish, "Multiple-channel detection using generalized coherence," in *Proc. IEEE Int. Conf. Acoust., Speech, Signal Process.*, Jun. 1990, vol. 5, pp. 2883–2886.

[6] A. Clausen and D. Cochran, "Non-parametric multiple channel detection in deep ocean noise," in *Proc. 31st Asilomar Conf. Signals, Syst. Comput.*, Oct. 1997, vol. 1, pp. 850–854.

[7] ——, "Asymptotic analysis of the generalized coherence estimate," *IEEE Trans. Signal Process.*, vol. 49, no. 1, pp. 45–53, Jan. 2001.

[8] D. Cochran, H. Gish, and D. Sinno, "A geometric approach to multiple-channel signal detection," *IEEE Trans. Signal Process.*, vol. 43, no. 9, pp. 2049–2057, Sep. 1995.

[9] K. Ghartey, A. Papandreou-Suppappola, and D. Cochran, "On the use of matching pursuit time-frequency techniques for multiple-channel detection," in *Proc. IEEE Int. Conf. Acoust., Speech, Signal Process.*, Salt Lake City, UT, May 2001, vol. 5, pp. 3201–3204.

[10] K. Ghartey, D. Cochran, and A. Papandreou-Suppappola, "Multichannel signal detection using time-varying estimation techniques," in *Proc. IEEE 6th Int. Symp. Signal Process. Applicat.*, Malaysia, Aug. 2001, vol. 2, pp. 577–580.

[11] K. Ghartey, "Applications of time-frequency techniques in multichannel signal detection," Master's thesis, Electrical Engineering Dept., Arizona State Univ., Tempe, AZ, May 2001.

[12] L. Cohen, *Time-Frequency Analysis*. Upper Saddle River, NJ: Prentice-Hall, 1995.

[13] P. Flandrin, *Time-Frequency/Time-Scale Analysis*. San Diego, CA: Academic, 1999, *Temps-fréquence*. Paris, France: Hermès, 1993, (original French ed.).

[14] A. Papandreou-Suppappola, Ed., *Applications in Time-Frequency Signal Processing*. Boca Raton, FL: CRC Press, 2002.

[15] S. Mallat and Z. Zhang, "Matching pursuit with time-frequency dictionaries," *IEEE Trans. Signal Process.*, vol. 41, no. 12, pp. 3397–3415, Dec. 1993.

[16] A. Bultan, "A four-parameter atomic decomposition of chirplets," *IEEE Trans. Signal Process.*, vol. 47, no. 3, pp. 731–745, Mar. 1999.

[17] R. Gribonval, "Sparse decomposition of stereo signals with matching pursuit and application to blind separation of more than two sources from a stereo mixture," in *Proc. Int. Conf. Acoust., Speech, Signal Process.*, Orlando, FL, 2002, vol. 3, pp. 3057–3060.

[18] R. Gribonval and E. Bacry, "Harmonic decomposition of audio signals with matching pursuit," *IEEE Trans. Signal Process.*, vol. 51, no. 1, pp. 101–111, Jan. 2003.

[19] M. R. McClure and L. Carin, "Matching pursuits with a wave-based dictionary," *IEEE Trans. Signal Process.*, vol. 45, no. 12, pp. 2912–2927, Dec. 1997.

[20] S. P. Ebenezer, A. Papandreou-Suppappola, and S. B. Suppappola, "Matching pursuit classification for time-varying acoustic emissions," in *Proc. 35th Asilomar Conf. Signals, Syst. Comput.*, Nov. 2001, vol. 1, pp. 715–719.

[21] S. P. Ebenezer, A. Papandreou-Suppappola, and S. B. Suppappola, "Classification of acoustic emissions using modified matching pursuit," *EURASIP J. Appl. Signal Process.*, pp. 347–357, Mar. 2004.

[22] X. Zhang, L. Durand, L. Senhadji, H. C. Lee, and J. L. Coatrieux, "Time-frequency scaling transformation of the phonocardiogram based of the matching pursuit method," *IEEE Trans. Biomed. Eng.*, vol. 45, pp. 972–979, Aug. 1998.

[23] A. Papandreou-Suppappola and S. B. Suppappola, "Adaptive time-frequency representations for multiple structures," in *Proc. IEEE Workshop Statist. Signal Array Process.*, Aug. 2000, pp. 579–583.

[24] ——, "Analysis and classification of time-varying signals with multiple time-frequency structures," *IEEE Signal Process. Lett.*, vol. 9, pp. 92–95, 2002.

[25] B. Boashash, "Estimating and interpreting the instantaneous frequency of a signal," *Proc. IEEE*, vol. 8, pp. 520–568, 1992.

[26] B. Barkat and B. Boashash, "Instantaneous frequency estimation of polynomial FM signals using the peak of the PWVD: Statistical performance in the presence of additive Gaussian noise," *IEEE Trans. Signal Process.*, vol. 47, no. 9, pp. 2480–2490, Sep. 1999.

[27] Z. M. Hussain and B. Boashash, "Adaptive instantaneous frequency estimation of multi-component FM signals," in *Proc. IEEE Int. Conf. Acoust., Speech, Signal Process.*, Istanbul, Turkey, Jun. 2000, pp. 657–660.

[28] V. Katkovnik and L. Stankovic, "Instantaneous frequency estimation using the Wigner distribution with varying and data-driven window length," *IEEE Trans. Signal Process.*, vol. 46, no. 9, pp. 2315–2325, Sep. 1998.
[29] V. Katkovnik, "Nonparametric estimation of instantaneous frequency," *IEEE Trans. Inf. Theory*, vol. 43, pp. 183–189, Jan. 1997.
[30] I. Djurovic and L. Stankovic, "Influence of high noise on the instantaneous frequency estimation using quadratic time-frequency distributions," *IEEE Signal Process. Lett.*, vol. 7, no. 11, pp. 317–319, Nov. 2000.
[31] A. Carlosena, C. Macua, and M. Zivanovic, "Instrument for the measurement of the instantaneous frequency," *IEEE Trans. Instrum. Meas.*, vol. 49, pp. 783–789, Aug. 2000.
[32] Z. M. Hussain and B. Boashash, "Multicomponent instantaneous frequency estimation: A statistical comparison in the quadratic class of time-frequency distributions," in *Proc. IEEE Int. Symp. Circuits Syst.*, 2001, vol. 2, pp. 109–112.
[33] J. E. Odegard, R. G. Baraniuk, and K. L. Oehler, "Instantaneous frequency estimation using the reassignment method," in *Proc. 68th SEG Meeting*, New Orleans, LA, 1998.
[34] L. F. Chaparro, R. Suleesathira, A. Akan, and B. Unsal, "Instantaneous frequency estimation using the discrete evolutionary transform for jammer excision," presented at the IEEE Int. Conf. Acoust., Speech, Signal Process., Salt Lake City, UT, May 2001.
[35] P. Loughlin, "Spectrographic measurement of instantaneous frequency and the time-dependent weighted average instantaneous frequency," *J. Acoust. Soc. Amer.*, vol. 105, pp. 264–274, 1999.
[36] M. Emresoy and A. El-Jaroudi, "Iterative instantaneous frequency estimation and adaptive matched spectrogram," *Signal Process.*, vol. 64, pp. 157–165, 1998.
[37] P. Duvaut, C. Veaux, A. Doucet, and P. Flandrin, "Instantaneous frequency estimation: Bayesian approach versus reassignment—Application to gravitational waves," in *Proc. IEEE Int. Conf. Acoustics, Speech, Signal Process.*, Atlanta, GA, 1996, vol. 5, pp. 2968–2971.
[38] T. A. C. M. Claasen and W. F. G. Mecklenbräuker, "The Wigner distribution—A tool for time-frequency signal analysis, Part I: Continuous-time signals," *Philips J. Res.*, vol. 35, pp. 217–250, 1980.
[39] R. A. Altes, "Wide-band, proportional-bandwidth Wigner-Ville analysis," *IEEE Trans. Acoust., Speech, Signal Process.*, vol. 38, pp. 1005–1012, Jun. 1990.
[40] A. Papandreou, F. Hlawatsch, and G. F. Boudreaux-Bartels, "The hyperbolic class of quadratic time-frequency representations, Part I: Constant-Q warping, the hyperbolic paradigm, properties, and members," *IEEE Trans. Signal Process. (Special Issue Wavelets Signal Process.)*, vol. 41, no. 12, pp. 3425–3444, Dec. 1993.
[41] S. M. Kay, *Fundamentals of Statistical Signal Processing; Estimation Theory*. Englewood Cliffs, NJ: Prentice-Hall, 1993, vol. 1.
[42] A. Papandreou-Suppappola, F. Hlawatsch, and G. F. Boudreaux-Bartels, "Quadratic time-frequency representations with scale covariance and generalized time-shift covariance: A unified hyperbolic, and power classes," *Digital Signal Process. Rev. J.*, vol. 8, pp. 3–48, 1998.

Kofi Ghartey was born in Ghana in 1978. He received the B.S. and M.S. degrees in electrical engineering from Arizona State University, Tempe, in 1999 and 2001, respectively.

In summer 2000, he held an internship position with GE Power Systems Energy Services.

Antonia Papandreou-Suppappola (S'91–M'95–SM'03) received the Ph.D. degree in electrical engineering from the University of Rhode Island, Kingston, in 1995.

She held a Navy-supported Research Faculty position at the University of Rhode Island. She is currently an Associate Professor at Arizona State University, Tempe. Her research interests are in the areas of time-frequency signal processing, integrated sensing and processing, and signal processing for wireless communications. She has published more than 80 refereed journal articles, book chapters, and conference papers.

Prof. Papandreou-Suppappola received the National Science Foundation CAREER Award in 2002. She is an Associate Editor of the IEEE TRANSACTIONS ON SIGNAL PROCESSING and Treasurer of the Conference Board of the IEEE Signal Processing Society.

Douglas Cochran (S'86–A'90–M'92–SM'96) received the S.M. and Ph.D. degrees in applied mathematics from Harvard University, Cambridge, MA, and degrees from the Massachusetts Institute of Technology, Cambridge, and the University of California, San Diego, in mathematics.

He has been on the Faculty of the Department of Electrical Engineering, Arizona State University (ASU), Tempe, since 1989 and is also affiliated with the Department of Mathematics and Statistics. Since May 2005, he has been Assistant Dean of Research in the Ira A. Fulton School of Engineering, ASU. Between 2000 and 2005, he was Program Manager for mathematics with the Defense Advanced Research Projects Agency (DARPA). Prior to joining ASU, he was a Senior Scientist with BBN Systems and Technologies Inc., during which time he was Resident Scientist with the DARPA Acoustic Research Center and the Naval Ocean Systems Center. He has been a Visiting Scientist at the Australian Defence Science and Technology Organisation. He has been a Consultant to several technology companies. His research is in applied harmonic analysis and statistical signal processing.

Prof. Cochran was General Cochair of the 1999 IEEE International Conference on Acoustics, Speech, and Signal Processing (ICASSP-99) and Cochair of the 1997 U.S.-Australia Workshop on Defense Signal Processing. He has also served as an Associate Editor for book series and journals, including the IEEE TRANSACTIONS ON SIGNAL PROCESSING.